RSC Advances

RSC Publishing

PAPER

View Article Online
View Journal | View Issue

Dielectric properties of silver nanoparticles coated with silica shells of different thicknesses†

Cite this: *RSC Advances*, 2013, **3**, 6964

Jose Enrico Q. Quinsaat,[ab] Frank A. Nüesch,[a] Heinrich Hofmann[b] and Dorina M. Opris*[a]

Received 5th December 2012,
Accepted 28th February 2013

DOI: 10.1039/c3ra23192e

www.rsc.org/advances

Core/shell nanoparticles having metallic silver nanoparticle cores of ~38 nm in diameter and silica shells of different thicknesses ranging from ~3.6–20 nm were prepared. For the silica coating, a slightly modified Stöber method was used which allowed preparing grams of core/shell nanoparticles for the first time. The particles were characterized by UV-vis spectroscopy, dynamic light scattering, scanning electron microscopy, transmission electron microscopy, and energy-dispersive X-ray scattering. Their dielectric properties were measured as pellets in parallel-plate capacitors. It was found that the permittivity is much influenced by the silica shell thickness with an increase in permittivity for thinner shells. A shell thickness of 20 ± 2 nm allowed fabrication of capacitors which have similar characteristics to those of silica, thus, there is no influence of the metal core on the dielectric properties anymore. However, by decreasing the silica shell to 17 ± 2, 8 ± 1.5, and 6.6 ± 1.5 nm the permittivity at high frequencies is increasing from 10, 34, to 41, respectively. The insulator to metal transition was observed for a silica shell thickness of 3.6 ± 1 nm. Functionalization of the silica surface with a hydrophobic coating removes surface adsorbed water as observed by the flat dielectric permittivity over a large frequency domain.

Introduction

Properties of metals change significantly when going from macroscopic to nanoparticle sizes.[1] In the last couple of years, much development has been done with respect to the synthesis of metal nanoparticles and some understanding of how to prepare different shapes and sizes has been achieved.[2] Blending such nanoparticles in polymeric, ceramic matrices allowed fabrication of new materials with unprecedented properties which might find their way in optical, electrical, and magnetic applications. Materials with high dielectric permittivity (ε') are of great interest for future electronic capacitors with high energy storage densities and low operating voltage.[3] For such applications not only high ε' is required, but also low conductivity and high breakdown field are desired properties. These two properties have a direct impact on the device lifetime and also on the maximum energy density of the capacitor which is given by:

$$U_e = \frac{1}{2}\varepsilon'\varepsilon_0 E_b^2$$

where ε' is the relative dielectric permittivity, E_b is the electric breakdown strength, and ε_0 the vacuum permittivity (8.85542×10^{-12} F/m).[3] The energy loss due to dissipation by the dielectric material is given by:

$$W = \pi\varepsilon' E f \tan\delta$$

where E is the electric field strength, f is the frequency, and $tan\delta$ is the loss factor. Thus a low dielectric loss material will have a low energy loss, especially for high frequency applications.

Several approaches have been used in order to produce materials with high ε' which include blends with highly polarizable ceramic particles,[4,5] polymers with polar functional groups,[6] and composite materials with conductive fillers.[7]

According to percolation theory, the effective ε' of composites increases rapidly at concentrations approaching the percolation threshold, when the conductive paths are hindered by a dielectric matrix.[8] Various conductive fillers like metal particles, conjugated polymers, or carbon black have been used for percolative composites with polymers as matrix materials.[9–13] However, although the reported ε' values were high, the blended materials showed high dielectric loss due to agglomeration of the fillers leading to conductive pathways. Several approaches were used to overcome this limitation. For example, Xu *et al.* used Al particles covered with an Al_2O_3

[a]*Swiss Federal Laboratories for Materials Science and Technology Empa, Laboratory for Functional Polymers, Ueberlandstr. 129, CH-8600, Dübendorf, Switzerland. E-mail: dorina.opris@empa.ch; Fax: +41 58 765 4012; Tel: +41 58 765 4304*
[b]*Ecole Polytechnique Fédérale de Lausanne (EPFL), Materials Institute, Powder Technology Laboratory (LTP), 1015 Lausanne, Switzerland*

† Electronic supplementary information (ESI) available: See DOI: 10.1039/c3ra23192e

insulating shell, and obtained composites with low dielectric losses.[14] Kempa *et al.* used silica coated conductive particles and observed that the shape and monodispersity of the nanoparticles strongly affect the dielectric properties of the composites. Li *et al.* used effective medium approximation of a composite made of three-phase material and showed that the effective ε' the breakdown strength, and the electrical energy density are strongly affected by the microstructure of the nanocomposite and therefore must be carefully controlled.[15]

From the literature, it became clear that in order to prepare reliable materials the percolation paths in composites containing conductive fillers should be avoided. This can be achieved by surrounding the particles with an insulating shell that precisely defines the minimum approach distance of twice the shell thickness (Fig. 1).[16]

Several approaches were already reported in the literature on how to prepare core/shell particles.[17] The most common one uses wet chemistry on preformed cores including interfacial polymerization of the shell onto the core, controlled phase separation techniques, and heterocoagulation.[18] Although high temperature formation of dielectric oxide shell is occasionally used, it is less attractive since the shell thickness is difficult to control.[19] Another way of preparing core/shell particles is by using layer by layer deposition.[20] Despite of these advances in the synthesis of core/shell particles, a challenge which still needs to be overcome is the up-scaling of the synthesis allowing preparation of sufficient material to be used for further investigations.

Despite of the large number of publications dealing with percolated materials, there is limited information on the ε' of monodisperse metal nanoparticles coated with an insulator shell of different thicknesses and/or composites of such well-defined particles in a matrix.

It is the aim of this work to prepare structurally well-defined core/shell particles having AgNP cores and silica as insulating shell (denoted as Ag@SiO_2(x), where x is the silica shell thickness taken from TEM measurements) and measure their dielectric properties as a function of shell thickness. Apart from many studies that concentrate on optical measurements with Ag@SiO_2 particles, dielectric measurements of such particles are not known. To be able to run such measurements large quantities of particles are required. Thus, a slightly modified Stöber method was developed that allowed us preparing grams of core/shell particles at higher concentrations as compared to the literature. The silica shells prevent the AgNPs from touching each other and also keep the AgNP cores at a defined minimum distance. The dielectric properties of such particles were measured for the first time in pellets in parallel-plate capacitors and the influence of the insulator shell thickness on the dielectric properties was investigated.

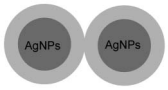

Fig. 1 Insulator shell (light grey) on conductive Ag nanoparticles (dark grey) defining the minimum distance between the cores as twice the shell thickness.

Experimental

Synthesis of Ag nanoparticles (38 nm)[21]

A solution of polyvinyl pyrrolidinone (PVP) (40.5 g, 361 mmol) in ethylene glycol (EG) was heated in a thermostat at 130 °C for 30 min. Then, a solution of Ag NO_3 (6 g, 36 mmol) dissolved in EG (4 mL) and nanopure water (3 mL) was added *via* rapid injection and the mixture was stirred at 130 °C for further 30 min. Afterwards, the mixture was cooled, washed with acetone, and centrifuged. The washing procedure was repeated twice before redispersion of the residue in ethanol (EtOH) (100 mL). AgNPs were prepared in 81% yield.

Synthesis of silica coated silver nanoparticles Ag@SiO_2(x nm)[22]

From the above dispersion of AgNPs in ethanol, 5 ml was taken and diluted with ethanol to 31.5 ml in order to obtain a conc. of 46 mM AgNPs. This dispersion was treated with NH_4OH (29%, 1.3 mL) under gentle stirring (see Table 1) at 25 °C followed by the dropwise addition of different concentrations of tetraethoxysilane (TEOS) in EtOH (3 mL) which was completed after 60 s (for concentrations see Table 1). The reaction mixture was stirred for further 20 h, then diluted with acetone, washed, centrifuged (4000 rpm, 45 min) and decanted. The washing procedure was repeated 3 times. The residue was redispersed in MeOH for further analysis. The particles were dried in high vacuum at 25 °C for 8 h.

Synthesis of hydrophobic coating: (Ag@SiO_2(17 nm)@alkylsilane)

Ag@SiO_2 (60 mg) was dispersed in EtOH (10 mL) and treated with dimethylamine (DMA) (40%, 166 μL, 1.34 mmol) under gentle stirring (500 rpm) followed by the dropwise addition of *n*-octyldimethylmethoxysilane (334 μL, 1.34 mmol) which was completed within a minute. The mixture was stirred for further 48 h, then diluted with acetone, washed, centrifuged (13 000 rpm, 25 min) and decanted followed by redispersion and further washing in isopropanol (13 000 rpm, 25 min) for 4 times. The particles were dried in high vacuum at 25 °C for 8 h.

Materials and methods

All chemicals were purchased from Aldrich and used as received.

Methods

The nanoparticles were observed by SEM on a Hitachi S-4800 and FEI NovaNanoSEM 230, TEM were done with Philips CM30 TEM and JEOL 2200FS TEM/STEM, UV-vis absorption spectra were recorded with a Cary 50 spectrophotometer, DLS were done with a Malvern Zetasized Nano ZS, FT-IR spectra were taken on a Bio-Rad FTS 6000 spectrometer, and ^{29}Si NMR spectra were recorded with a Bruker Avance-400 spectrometer.

Table 1 Amount of reagents used for the coating of AgNPs with different thickness silica shell

Sample $Ag@SiO_2(x \pm y$ nm)[a]	Vol% TEOS in EtOH [3 mL][e]	Particles size by TEM	Particles size by DLS
$Ag@SiO_2(20 \pm 2$ nm)[b]	20%	78	79
$Ag@SiO_2(17 \pm 2$ nm)[b]	15%	72	72
$Ag@SiO_2(8 \pm 1.5$ nm)[c]	8%	54	57
$Ag@SiO_2(6.6 \pm 1.5$ nm)[c]	5%	51	54
$Ag@SiO_2(3.6 \pm 1$ nm)[d]	2.5%	45	366

[a] Where x is the silica shell thickness and y is the deviation of the silica shell from TEM. [b] Stirring rate 550 rpm. [c] Stirring rate 500 rpm. [d] Stirring rate 400 rpm. [e] 31.5 ml of 46 mM AgNP dispersed in ethanol was used.

Image analysis was used for the TEM micrographs to estimate the particles size of about 400 Ag cores by using ImageJ and a ruler for Windows was used to calculate the shells of about 100 coated particles. Permittivity measurements were done in the frequency range of 100 Hz to 1 MHz using an HP 4284A LCR meter. The amplitude of the probing ac electric signal applied to the samples was 1 V. The permittivity was determined from the capacitance: $C = \varepsilon\varepsilon_0 A/d$, where A is the electrode area, d is the thickness of the capacitor, and ε_0 is the vacuum permittivity. Before use, the samples were dried for 8 h at 2×10^{-2} mbar. Pellets were prepared by pressing at 3 tons (Ø = 3 mm) and were then covered with silver paste electrodes. Their microstructures were measured with SEM (see ESI†). All the samples were measured immediately after pellet preparation in order to avoid changes in the water content.

Results

Synthesis and characterization of AgNPs coated with SiO_2

A wide range of different shapes and sizes of AgNPs have been prepared including sphere, spheroid, cube, octahedron, tetrahedron, bipyramid, rod, and wire starting from cheap and readily available silver salts.[23] For a general overview of the state of the art on the shape controlled syntheses of AgNPs the reader is referred to the excellent review article by Xia *et al.*[24] The most common way for preparing AgNPs includes the reduction of silver salt by boron hydrides, polyols, or hydrogen.[25]

We prepared AgNPs by reduction of $AgNO_3$ with EG in the presence of PVP as capping agent at 130 °C. The particles were stabilized by polyvinylpyrrolidone (PVP). The reactions were initially done on a small scale (0.2 g $AgNO_3$), however in order to be able to make dielectric investigations of AgNPs, quantities in the g range are required. Thus, the possibility of up-scaling the synthesis was investigated. Since the reaction temperature influences particles size, an accurate control of the temperature was required. In order to achieve this, a reactor heated with a thermostat was used. This setup enabled control within ±1 °C during the synthesis. Fig. 2 shows the TEM images of the prepared AgNPs on 6 g scale. By TEM it was found that the average particles size was about 38 ± 2 nm in diameter and by DLS that they have a reasonable size distribution (0.2).

Silica is well known for its good insulator properties. Core/shell particles with SiO_2 shell having controllable thickness were prepared by the Stöber method.[26] This layer by layer technique was intensely used for example to prepare polystyrene-silica, gold-silica core/shell particles with controlled shell thickness from a few nanometers to several hundreds.[27]

Ag particles[28] and nanowires[29] were also coated with amorphous silica shells of different thickness by using TEOS as silica precursor. We also used Stöber method for the silica coating of AgNPs. The silica shells not only hinder agglomeration of AgNPs and enhance their stability, but also allow for surface functionalization.[30] In a typical synthesis, the AgNPs are dispersed at a certain concentration in ethanol and TEOS is hydrolyzed and deposited on the surface of the nanoparticles. A disadvantage of Stöber method is the high dilution required (typical concentration range from 0.01 mM to 1 mM) which made up-scaling of the process unpractical. We therefore slightly modified the reaction conditions and systematically increased the concentration of AgNPs (46 mM) such that about 0.1 g of AgNPs per batch was coated. The strong contrast between the black silver core and the gray shell in the TEM images (Fig. 3) confirms that core/shell nanoparticles formed. Despite the use of NH_4OH which was thought to trigger the dissolution of the silver cores, no core-free silica shells were observed in the TEM images. In comparison, the use of DMA as catalyst for the hydrolysis of TEOS did not give uniform and spherical silica shells as suggested in the literature.[31]

Furthermore, the presence of the silica shell was confirmed by EDX done on the naked AgNPs and on the coated particles as shown in Fig. 4. Only in the latter spectrum, silicon is detected. The Cu and C peaks correspond to the carbon-coated copper grid on which the particles were deposited for this test.

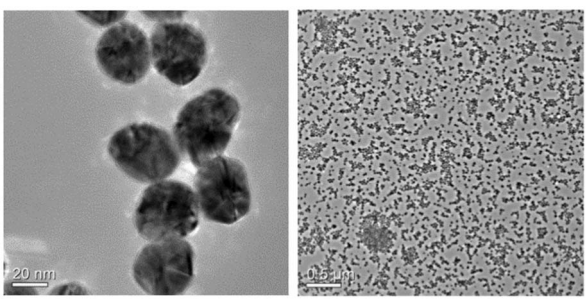

Fig. 2 TEM images of AgNPs prepared by reduction of $AgNO_3$ with ethylene glycol. The reaction was done starting with 6 g $AgNO_3$.

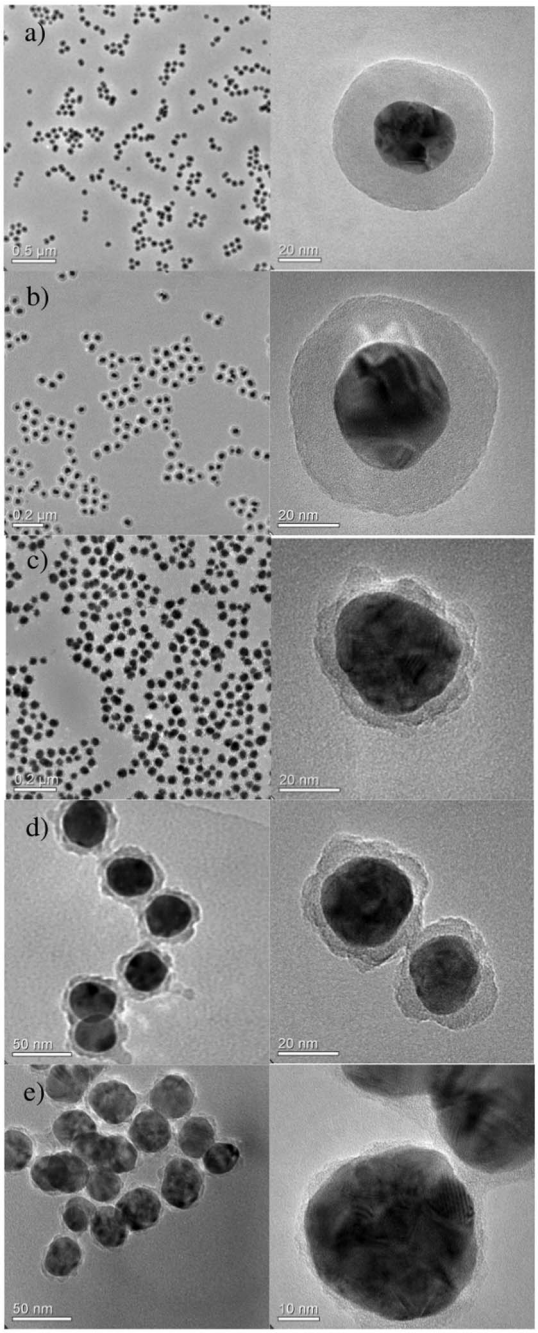

Fig. 3 TEM images of the AgNPs coated with a silica shell. The average diameters of AgNPs were 38 nm while the SiO_2 shells were about 20 ± 2 nm (a); 17 ± 2 nm (b); 8 ± 1.5 nm (c); 6.6 ± 1.5 nm (d); 3.6 ± 1 nm (e).

The silica shell thickness could be varied by altering the initial TEOS concentration. The growth of very thin silica shells requires slow and careful addition of TEOS into the solution.[32] The silica shell grown on the silver nanoparticles was quite uniform and also spherical in shape when the shell thickness was about 17 nm or higher, but was less uniform for the thinner shells. This effect was also observed by others. For example Yin *et al.* coated Ag nanowires and found that when a thin silica shell of about 2 nm was formed, the thickness of the

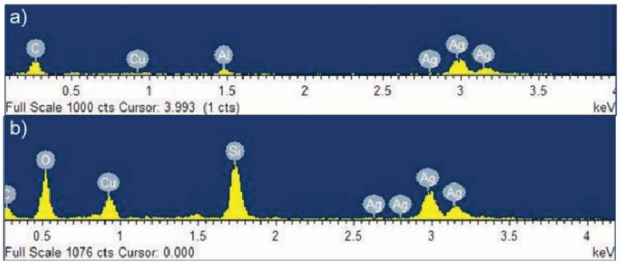

Fig. 4 EDX of the naked AgNPs (a) and of the AgNPs coated with SiO_2 (b).

shell varied considerably. Thicker shells were smoother and more uniform.[29] It was also observed that the specific morphology of the particles is preserved in the coating process. Graf *et al.* used PVP adsorbed on various colloidal particles and coated these particles with silica shells of variable thickness. The length of the polymer used strongly influenced the homogeneity and the smoothness of the initial silica coating.[33] Fig. 3 shows TEM images of AgNPs with SiO_2 shells of different thickness. Additionally, the TEM images clearly show that the SiO_2 shell thickness can be changed by altering the amount of TEOS used.

The surface plasmon resonance of AgNPs is sensitive to size, shape, and the dielectric material surrounding the nanoparticles. While the naked Ag particles give rise to an absorption peak at λ = 415 nm, a small bathochromic shift (Fig. 5) with increasing the silica shell from 425 nm for 6.6 nm particles to 437 nm for 20 nm particles was observed. This can be explained by the change of the surrounding medium of the AgNPs, since silica possesses a higher refractive index than the solvent (MeOH). When the silica shell thickness was reduced to around 3.6 nm, the UV-vis spectrum featured broadened peaks. For the thicker shells, silica is completely covering the AgNPs. Because of the basic conditions, the surface hydroxyl groups are deprotonated and therefore electrostatic stabilization is the mechanism preventing agglomeration. The nanoparticles with thin and partial silica coating behave like conventional hard spheres in a Lennard–Jones potential and therefore aggregate. We assume that the surface coverage with silica is patchy and that agglomeration comes about by contact between particles at the surface parts which either have a very

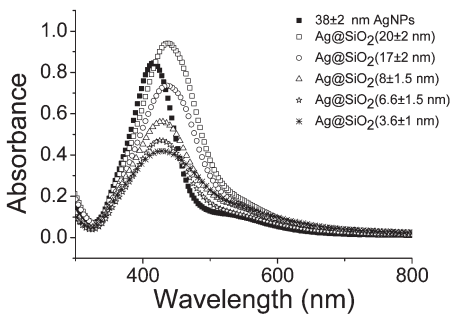

Fig. 5 UV-vis absorption spectra of AgNPs and of AgNPs coated with a silica shell. A small bathochromic shift can be seen with increasing shell thickness.

thin silica layer or are even free of silica. Then van der Waals forces are strong and result in agglomeration. Whether there is any residual PVP on the surface with little or no silica cannot be said at present.

The size increases with increasing the silica shell is also reflected by DLS and further confirms the coating (Fig. 6). Interestingly, while almost all dispersed particles have similar sizes as those determined by TEM, the size of $Ag@SiO_2$(3.6 ± 1) with a TEM diameter of 45 nm appears much larger (Table 1) a sign for agglomerated particles. A direct comparison of our results with the literature is not possible since no DLS data are given for metal particles coated with a silica shell.

Dielectric properties of $Ag@SiO_2$ in pressed pellets

The real part of the dielectric function ε' of pressed pellets of powder samples composed of $Ag@SiO_2$ nanoparticles were obtained by measuring the capacitance of the pellets using the sandwich architecture $Ag/Ag@SiO_2/Ag$ in the frequency range of 100 Hz to 1 MHz (see Experimental). The dielectric response of $Ag@SiO_2$ pellets is given in Fig. 7. As expected, an increase in ε' with decreasing shell thickness was observed at all frequencies. Concretely, for shell thicknesses of 20 ± 2, 17 ± 2, 8 ± 1.5, and 6.6 ± 1.5 nm ε'-values of 4.6, 10, 34 and 41, respectively, were obtained. AgNPs coated with a very thin insulating shell of about 3.6 ± 1 nm were conductive and it was not possible to run the dielectric measurement. For thicker shells, the ε' of $Ag@SiO_2$ pellets is almost constant at high frequencies but increases at lower frequencies. The reason for this might be due to the presence of traces of ions and residual water absorbed on the silica surface which is rather difficult to remove which would increase the ion conductivity at low frequencies.

In order to exclude traces of water which may have caused the ε' values to scatter, the powder sample of AgNPs with a shell thickness of 17 ± 2 nm was hydrophobized with a silane reagent. The wettability test done in water/toluene as well as the presence of the signal at δ = 13 ppm in the ^{29}Si NMR spectrum characteristic for the Si–C are clear indications that the silylation was successfully achieved (see ESI†). The dielectric properties of silylated sample showed ε' values that remained constant even at lower frequencies (Fig. 8). As mentioned before, the rising permittivity of the non-silylated nanoparticle samples is likely to be due to ionic impurity conduction which is favored by water adsorption in the porous

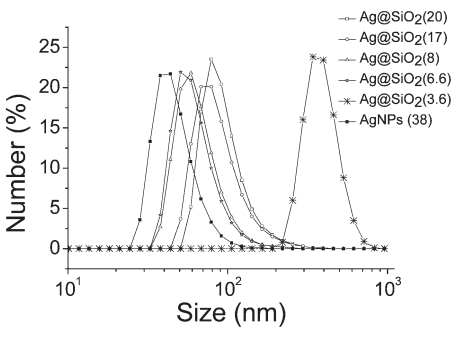

Fig. 6 Hydrodynamic diameter D_H determined by DLS of AgNPs before and after coating with silica shell. An increase in particle size is observed with increasing shell thickness, except for the D_H-value of which does not match single particle size. For explanation, see text.

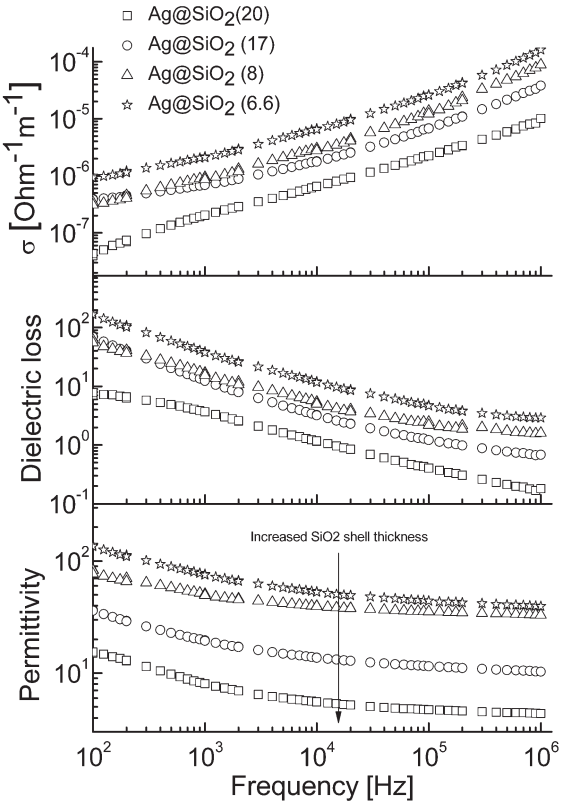

Fig. 7 Permittivity, dielectric loss, and conductivity of AgNPs coated with silica shells of different thickness as function of frequency.

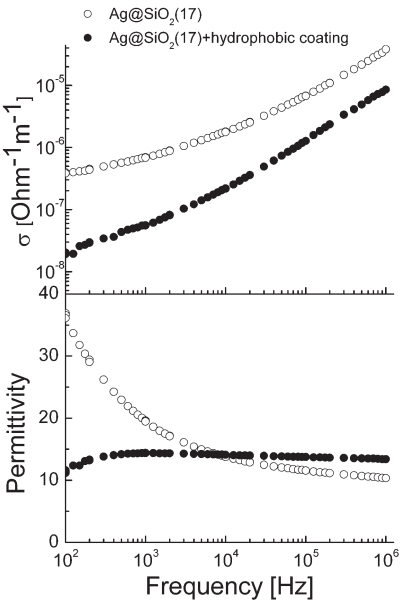

Fig. 8 Permittivity and conductivity of AgNPs coated with a 17 ± 2 nm silica shell and of a silica hydrophobized with a silane reagent.

nanoparticle film. Silylation creates a hydrophobic shell around the Ag nanoparticles and removes the water from the surface. At high frequencies, typically above 10^4 Hz, the ion conduction mechanism no longer contributes to the permittivity of the nanoporous samples. The difference between silylated and non-silylated samples in the high frequency region is rather small and is attributed to slightly different packing of the nanoparticle in the pellets and to the experimental uncertainty. Since the ε' of air is rather low, and the air voids are filled by alkyl chains which have a ε' of about 2, a slight increase in the ε' should be observed for the hydrophobized sample. Such effect was observed by others. For example the permittivity value of 80 of bulk TiO_2 decreased to 58 for TiO_2 nanoparticles due to the presence of voids.[34]

The dielectric loss increases with the thinning of silica shell (Fig. 7). This loss of charges is also reflected by the conductivity of the samples. The AC conductivity is given by $\sigma = 2\pi\upsilon\varepsilon_0\varepsilon''$ where ε'' is the imaginary part of the complex dielectric function ε', ε_0 is the permittivity of vacuum and υ is the frequency. If the universal response function $\sigma(\upsilon) = A\,\upsilon^s$ is fitted to the measured AC conductivity (Fig. 7), a frequency exponent between 0.49 and 0.56 is obtained, depending on the thickness of the silica shell.[35] A frequency exponent $s < 1$, is typical for non-Debye type relaxation caused by hopping or tunnelling of charges.[36] The trend that s decreases with decreasing the silica shell thickness is characteristic for a system in which conductivity increases.[37] Through the hydrophobization of the silica surface the conductivity of the sample decreases significantly at all frequencies as compared to the sample where no hydrophobic coating was used. Hydrophobization of the silica surface is required not only to stabilize the dielectric properties of the $Ag@SiO_2$ but it helps to compatibilize the particles with an organic matrix where such particles could be used as high ε' filler. Further work is presently going in this direction.

Our samples can be considered as percolating conductive particles held apart by the twice the thickness of the insulating shell. If we do not have water inclusion in our pellet samples, the voids can be considered to be filled with air. Therefore the calculation of the effective electrical permittivity of the samples amounts to calculation of highly concentrated core-shell particles in an air matrix ($\varepsilon_m = 1$). It is well known that only effective medium theories such as the one derived by Bruggemann can reasonably well describe non-dilute particle inclusion in a matrix.[38] Here we applied an effective-medium theory that has been developed for two-phase random composites with an interfacial shell given by[39]:

$$(1-F)\frac{\varepsilon_{eff}-\varepsilon_m}{2\varepsilon_{eff}+\varepsilon_m}+F\frac{\varepsilon_{eff}-\varepsilon_c}{2\varepsilon_{eff}+\varepsilon_c}=0$$

$$\varepsilon_{eff}=\frac{F(3\varepsilon_c-3\varepsilon_m)+2\varepsilon_m-\varepsilon_c+\sqrt{[F^2(9\varepsilon_m^2-18\varepsilon_c\varepsilon_m+9\varepsilon_c^2)-F(12\varepsilon_m^2-18\varepsilon_c\varepsilon_m+6\varepsilon_c^2)+4\varepsilon_m^2+4\varepsilon_c\varepsilon_m+\varepsilon_c^2]}}{4}$$

with

$$\varepsilon_c=\varepsilon_1\frac{2\varepsilon_1+\varepsilon_2+2\alpha(\varepsilon_2-\varepsilon_1)}{2\varepsilon_1+\varepsilon_2-\alpha(\varepsilon_2-\varepsilon_1)}$$

where ε_{eff} is the effective permittivity, ε_1 the permittivity of the shell (ε_{silica} = 3.9), ε_2 the permittivity of the core (ε_{Ag} = 10 000),[40] ε_c the dielectric permittivity of the core-shell particles, α is the volume fraction of core in the core-shell particles $\alpha = (r_0/R)^3$, where r_0 is the radius of Ag nanoparticles and R is the radius of the core-shell particles. For the calculations ideal spheres were used. Their closed-packed arrangement (hcp) leads to volume fraction F of 74%. Given the deviation of the experimental particles from spherical structure it is difficult to indicate a precise packing density. From the SEM images of pellets (see ESI†) we infer a tight packing. Therefore we have chosen the highest packing density that can be achieved with identical spheres. The calculated and measured effective permittivity as a function of shell thickness is displayed in Table 2. The measured values are clearly larger than the calculated ones which could be due to the failure of the model at the percolation limit, even though the theory proved to fit the permittivity of polymer composites with a volume fraction of $BaTiO_3$ particles up to 70% or might be due to traces of water that are rather hard to remove.

Conclusions

We report an upscale of the synthesis of Ag nanoparticles of 38 nm size as well as their coating with a silica shell of different thicknesses by the Ströber method. The silica shell was varied from ~3.6 nm to 20 nm. The core/shell structure of the prepared particles was clearly proven by using a combination of techniques: UV-vis, DLS, SEM, TEM, and EDX. Parallel-plate capacitors of pellets composed of pressed powder of Ag nanoparticles coated with different silica shells were made and the dielectric properties were investigated as function of the shell thickness. For a shell of 3.6 ± 1 nm, the insulator layer is too thin and the particles are conductive while increasing the shell thickness to 6.6 ± 1.5 nm, a shift from conductive to dielectric behaviour was observed. A further increase in the shell to 20 ± 2 nm hides the presence of the metal core and the resulting particles behave similar to silica. The conductivity of the samples due to absorbed water on the silica surface can be reduced by hydrophobization of the surface with an alkyl silane. Such hydrophobized particles have high permittivity, small dielectric losses, and are ready dispersible in nonpolar solvents and are therefore attractive fillers particularly for polydimethylsiloxane material for

Table 2 The calculated and measured ε' for different silica thicknesses

Entry	ε_{eff}' calc.[a]	$\varepsilon'_{measured}$[b]
$Ag@SiO_2(20)$	3.9	4.6
$Ag@SiO_2(17)$	4.2	10
$Ag@SiO_2(8)$	6.9	34
$Ag@SiO_2(6.6)$	8.0	41
$Ag@SiO_2(3.6)$	13.5	conductive

[a] $\varepsilon_m = 1$ for air, $\varepsilon'_{SiO2} = 3.9$ [b] In order to avoid ionic conductivity contributions, the permittivity at the frequency of 10^4 Hz is given.

transducer and more generally for large energy storage capacitors.

Acknowledgements

We gratefully acknowledge D. Schreier for helping with the TEM and SEM measurements, Dr F. La Mattina for providing us with the infrastructure for the impedance measurements, Dr D. Rentsch for the ^{29}Si NMR measurement (all Empa), and B. Sinnet from Eawag for helping with DLS measurement. We also gratefully acknowledge Swiss National Science Foundation (SNF132101) and Swiss Federal Laboratories for Materials Science and Technology (Empa, Dübendorf) for financial support.

Notes and references

1 (*a*) K. L. Kelly, E. Coronado, L. L. Zhao and G. C. Schatz, *J. Phys. Chem. B*, 2003, **107**, 668–677; (*b*) A. E. Welles, *Silver nanoparticles properties, characterization and applications*, Nova Science Pub. Inc., New York, 2012; (*c*) A. P. Alivisatos, *Science*, 1996, **271**, 933; (*d*) C. J. Murphy and N. R. Jana, *Adv. Mater.*, 2002, **14**, 80.

2 J. Zeng, X. Xia, M. Rycenga, P. Henneghan, Q. Li and Y. Xia, *Angew. Chem. Int. Ed.*, 2011, **50**, 244–249.

3 (*a*) N. Guo, S. A. Di Benedetto, P. Tewari, M. T. Lanagan, M. A. Ratner and T. J. Marks, *Chem. Mater.*, 2010, **22**, 1567–1578; (*b*) J. Pan, K. Li, J. Li, T. Hsu and Q. Wang, *Appl. Phys. Lett.*, 2009, **95**, 022902; (*c*) J. Claude, Y. Lu, K. Li and Q. Wang, *Chem. Mater.*, 2008, **20**, 2078–2080; (*d*) B. Chu, X. Zhou, K. Ren, B. Neese, M. Lin, Q. Wang, F. Bauer and Q. M. Zhang, *Science*, 2006, **313**, 334–336.

4 (*a*) Y. Bai, Z.-Y. Cheng, V. Bharti, H. S. Xu and Q. M. Zhang, *Appl. Phys. Lett.*, 2000, **76**, 3805; (*b*) J. Li, S. Seok, B. Chu, F. Dogan, Q. Zhang and Q. Wang, *Adv. Mater.*, 2009, **21**, 217–221; (*c*) G. Gallone, F. Carpi, D. De Rossi, G. Levita and A. Marchetti, *Mat. Sci. Eng.*, 2007, **C 27**, 110–116; (*d*) H. Stoyanov, M. Kollosche, S. Risse, D. N. McCarthy and G. Kofod, *Soft Matter*, 2011, **7**, 194.

5 Z. Li, L. A. Fredin, P. Tewari, S. A. DiBenedetto, M. T. Lanagan, M. A. Ratner and T. J. Marks, *Chem. Mater.*, 2010, **22**, 5154–5164.

6 P. Hedvin, *Dielectric spectroscopy of polymers*, Adam Higler LTD, Budapest, 1977.

7 (*a*) C. Huang and Q. Zhang, *Adv. Funct. Mater.*, 2004, **14**, 501–506; (*b*) S. Kirkparck, *Rev. Mod. Phys.*, 1973, **45**, 574; (*c*) C. W. Nan, *Prog. Mater. Sci.*, 1993, **37**, 1; (*d*) C. Pecharroman and J. S. Moya, *Adv. Mater.*, 2000, **12**, 294; (*e*) Z.-M. Dang, Y. Shen and C. W. Nan, *Appl. Phys. Lett.*, 2002, **81**, 4814.

8 C. Pecharroman and J. S. Maya, *Adv. Mater.*, 2000, **12**, 294.

9 (*a*) Y. Rao, C. P. Wong and J. Xu, *US Pat.*, 6864306, 2005; (*b*) H. W. Choi, Y. W. Heo, J. H. Lee, E. T. Park and Y. K. Chung, *Appl. Phys. Lett.*, 2006, **89**, 132910; (*c*) J. Lu, K. S. Moon, J. Xu and C. P. Wong, *J. Mat. Chem.*, 2006, **16**, 1543.

10 L. Qi, B. I. Lee, S. Chen, W. D. Samuels and G. J. Exarhos, *Adv. Mater.*, 2005, **17**, 1777–1781.

11 Y. Shen, Y. Lin, M. Lij and C. W. Nan, *Adv. Mat.*, 2007, **19**, 1418.

12 T. Kempa, D. Carnahan, M. Olek, M. Correa, M. Giersig, M. Cross, G. Benham, M. Sennett, Z. Ren and K. Kempa, *J. Appl. Phys.*, 2005, **98**, 034310.

13 T. I. Yang, R. N. C. Brown, L. C. Kempel and P. Kofinas, *Nanotech.*, 2011, **22**, 105601.

14 J. Xu and C. P. Wong, *Appl. Phys. Lett.*, 2005, **87**, 082907.

15 J. Y. Li, L. Zhang and S. Ducharme, *Appl. Phys. Lett.*, 2007, **90**, 132901.

16 D. Wilkinson, J. S. Langer and P. N. Sen, *Physical Review B*, 1983, **28**, 1081–1087.

17 (*a*) H. Goh, H.-J. Lee, B. Nam, Y. B. Lee and W. S. Choi, *Chem. Mat.*, 2011, **23**, 4832–4837; (*b*) O. Niitsoo and A. Couzis, *J. Coll. Interf. Sci*, 2011, **354**, 887–890; (*c*) A. M. Schmidt, *Macromol. Rapid Commun.*, 2005, **26**, 93–97; (*d*) H. Li, J. Han, A. Panioukhine and E. Kumacheva, *J. Coll. Interf. Sci.*, 2002, **255**, 119–128; (*e*) H. Li, J. Han, A. Panioukhine and E. Kumacheva, *J. Coll. Interf. Sci.*, 2002, **255**, 119–28; (*f*) N. Vogel, C. Fernandez-Lopez, C. J. Perez-Juste, L. M. Liz-Marzan, K. Landfester and C. K. Weiss, *Langmuir*, 2012, **28**, 8985–8993.

18 H. H. Pham and E. Kumacheva, *Macromol. Symp.*, 2003, **192**, 191–205.

19 (*a*) G. P. Burns, *J. Appl. Phys.*, 1988, **65**, 2095–2097; (*b*) J. Biener, E. Farfan-Arriba, M. Bienel, C. M. Friend and R. J. Madix, *J. Chem. Phys.*, 2005, **123**, 094705–1-094705-6.

20 (*a*) W. Ströber, A. Fink and E. Bohn, *J. Colloid Interface Sci.*, 1968, **26**, 62; (*b*) A. Guerrero-Martinez, J. Perez-Juste and L. M. Liz-Marzan, *Adv. Mater.*, 2010, **22**, 1182; (*c*) M. Iijima and H. Kaniya, *Langmuir*, 2010, **26**, 17943–17948; (*d*) C. Fernandez-Lopez, C. Mateo-Mateo, R. A. Alvarez-Puebla, J. Perz-Juste, I. Pastoriza-Santos and L. M. Liz-Marzan, *Langmuir*, 2009, **25**, 13894.

21 (*a*) B. J. Wiley, S. H. Im, Z. Y. Li, J. McLellan, A. Siekkinen and Y. Xia, *J. Phys. Chem. B*, 2006, **110**, 15666–15675; (*b*) D. Kim, S. Jeong and J. Moon, *Nanotechnology*, 2006, **17**, 4019–4024.

22 (*a*) H. Baida, P. Billaud, S. Marhaba, D. Christofilos, E. Cottancin, A. Crut, J. Lermeé, P. Maioli, M. Pellarin, M. Broyer, N. Del Fatti and F. Valleée, *Nano Letters*, 2009, **9**, 3463–3469; (*b*) F. Zhang, G. Braun, Y. Shi, Y. Zhang, X. Sun, N. Reich, D. Zhao and G. Stucky, *J. Am. Chem. Soc.*, 2010, **132**, 2850–2851.

23 (*a*) Y. Xia, Y. Xiong, B. Lim and S. E. Skrabalak, *Angew. Chem. Int. Ed.*, 2009, **48**, 60; (*b*) S. H. Im, Y. T. Lee, B. Wiley and Y. Xia, *Angew. Chem.*, 2005, **117**, 2192; (*c*) D. Yu and V. W.-W. Yam, *J. Am. Chem. Soc.*, 2004, **126**, 13200.

24 Y. Xia, Y. Xiong, B. Lim and S. E. Skrabalak, *Angew. Chem. Int. Ed.*, 2009, **48**, 60–103.

25 (*a*) A. R. Siekkinen, J. M. McLellan, J. Chen and Y. Xia, *Chem. Phys. Lett.*, 2006, **432**, 491; (*b*) D. D. Evanoff and G. Chumanov, *J. Phys. Chem. B*, 2004, **108**, 13948.

26 W. Ströber, A. Fink and E. Bohn, *J. Colloid Interface Sci.*, 1968, **26**, 62.

27 (*a*) F. Caruso, R. A. Caruso and H. Möhwald, *Science*, 1998, **282**, 1111; (*b*) Y. Lu, J. McLellan and Y. Xia, *Langmuir*, 2004, **20**, 3464.

28 (*a*) K. Xu, J.-X. Wang, X.-L. Kang and J.-F. Chen, *Mat. Lett.*, 2009, **63**, 31–33; (*b*) H. Baida, P. Billaud, S. Marhaba, D. Christofilos, E. Cottancin, A. Crut, J. Lerme, P. Maioli, M. Pellarin, M. Broyer, N. Del Fatti and F. Vallee, *Nano Lett.*, 2009, **9**, 3463–3469; (*c*) T. Ung, L. M. Liz-Marzan and P. Mulvaney, *Langmuir*, 1998, **14**, 3740–3748; (*d*) V.

V. Hardikar and E. Matijevic, *J. Colloid Interace. Sci.*, 2000, **221**, 133–136; (*e*) Y. Kobayashi, Y. H. Katakami, E. Mine, D. Nagao, M. Konno and L. M. Liz-Marzan, *J. Colloid. Interface Sci.*, 2005, **283**, 392–396; (*f*) Y. Han, J. Jiang, S. S. Lee and J. Y. Ying, *Langmuir*, 2008, **24**, 5842–5848.

29 Y. Yin, Y. Lu, Y. Sun and Y. Xia, *Nano Lett.*, 2002, **2**, 427–430.

30 Q. Kong, X. Yu, X. Zhang, H. Du and H. Gong, *J. Mater. Chem.*, 2012, **22**, 7767–7774.

31 Y. Kobayashi, V. Katakami, E. Mine, D. Nagao, M. Konno and L. M. Liz-Marzan, *J. Colloid Interface Sci.*, 2005, **283**, 392–396.

32 J. Yang, F. Zhang, Y. Chen, S. Qian, P. Hu, W. Li, Y. Deng, Y. Fang, L. Han, M. Luqman and D. Zhao, *Chem. Commun.*, 2011, **47**, 11618–11620.

33 C. Graf, D. L. J. Vossen, A. Imhof and A. van Blaaderen, *Langmuir*, 2003, **19**, 6693.

34 B. Balasubramanian, K. L. Kraemer, N. A. Reding, R. Skomski, S. Ducharme and D. J. Sellyer, *ASC Nano*, 2010, **4**, 1893–1900.

35 (*a*) M. M. Ahmad, S. A. Makhlouf and K. M. S. Khalil, *J. Appl. Phys.*, 2006, **100**, 094232; (*b*) G. Garcia-Belmonte, V. Kytin, T. Dittrich and J. Bisquert, *J. Appl. Phys.*, 2003, **94**, 155262.

36 A. K. Jonscher, *Nature*, 1977, **267**, 673.

37 S. R. Elliott, *Adv. Phys.*, 1987, **36**, 135.

38 W. R. Tinga, in "*Progress in Electromagnetics Research; Dielectric Properties of Heterogeneous Materials*", ed. J. A. Kong, A. Priou, Elsevier Science Publishing Co. Inc., New York, 1992, p. 1–12.

39 Q. Xue, *J. Mater. Sci. Technol.*, 2000, **16**, 367–369.

40 D. R. Bowman and D. Strout, *Phys. Rev. B*, 1989, **40**, 7. For metal insulator composites, the permittivity diverges close to the percolation threshold of the metallic fillers. In order to reflect this behavior using the effective medium theory applied in our paper, an infinite value for ε_{Ag} would have to be chosen. Here, an arbitrary high enough ε_{Ag} number that yields the same results as an infinite ε_{Ag} value was chosen.